articles

molecular pharmaceutics

Direct Measurement of Nucleoside Monophosphate Delivery from a Phosphoramidate Pronucleotide by Stable Isotope Labeling and LC−ESI⁻-MS/MS

Jisook Kim, Tsui-fen Chou, George W. Griesgraber, and Carston R. Wagner*

Department of Medicinal Chemistry, College of Pharmacy, University of Minnesota, Minneapolis, Minnesota 55455

Received December 24, 2003

Abstract: Amino acid phosphoramidates of nucleosides have been shown to be potent antiviral and anticancer agents with the potential to act as nucleoside monophosphate prodrugs. To access their ability to deliver 3′-azido-3′-deoxythymidine (AZT) 5′-monophosphate to cells, the decomposition pathway of an ^{18}O-labeled AZT amino acid phosphoramidate was investigated by capillary reverse-phase high-performance liquid chromatography interfaced with negative ion electrospray ionization mass spectrometry (LC−ESI⁻-MS/MS). ^{18}O-labeled L-AZT tryptophan phosphoramidate methyl ester ([^{18}O]**2**) was synthesized with an $^{18}O/^{16}O$ relative ratio of 1.22 ± 0.18. For CEM cells, a human T-lymphoblast leukemia cell line, incubated with [^{18}O]**2**, values of 1.55 ± 0.37, 0.34, and 0.13 were found for the $^{18}O/^{16}O$ relative ratio of intracellular AZT-MP for time intervals of 0.5, 4, and 20 h, respectively. The decrease in the level of labeled AZT-MP in CEM cells corresponded to a rapid increase in the amount of intracellular AZT presumably by dephosphorylation of AZT-MP. In contrast, for peripheral blood mononuclear cells (PBMCs), the $^{18}O/^{16}O$ relative ratio values of intracellular AZT-MP were 1.43, 1.06, and 0.61 for time intervals of 0.5, 4, and 20 h, respectively. Intracellular AZT in PBMCs was nearly undetectable for each time interval. Taken together, these results are consistent with the detection of direct P−N bond cleavage by CEM cells and PBMCs. However, AZT phosphoramidates are able to more effectively deliver AZT-MP to PBMCs than to CEM cells. Differential expression of 5′-nucleotidase in CEM cells relative to PBMCs is likely the reason for this discrepancy. Although applied to a phosphoramidate pronucleotide, the judicious use of ^{18}O labeling and LC−MS is a general approach that could be applied to the investigation of the intracellular fate of other pronucleotides.

Keywords: Prodrugs; antiviral agent; AZT; phosphoramidate

Introduction

Nucleosides make up an important class of antiviral and anticancer therapeutics. In general, the biological activity of nucleosides is dependent on their ability to be converted intracellularly to the corresponding mono-, di-, and triphosphates by cellular kinases.[1] Consequently, the substrate specificity of these enzymes has restricted the potential biological activity of these compounds. In addition, the long-term administration of nucleoside-based drugs can result in decreased kinase activity, thus reducing their efficacy. For example, resistance to the antiviral activity of 3′-azido-3′-deoxythymidine (AZT),[2,3] 2′,3′-dideoxycytidine (ddC),[4] and acyclovir (ACV)[5,6] has been shown to arise from the

* To whom correspondence should be addressed: Department of Medicinal Chemistry, College of Pharmacy, University of Minnesota, Minneapolis, MN 55455. Telephone: (612) 625-2614. Fax: (612) 624-0139. E-mail: wagne003@tc.umn.edu.

(1) Balzarini, J. Metabolism and mechanism of antiretroviral action of purine and pyrimidine derivatives. *Pharm. World Sci.* **1993**, 113−126.

10.1021/mp0340338 CCC: $27.50
Published on Web 02/03/2004

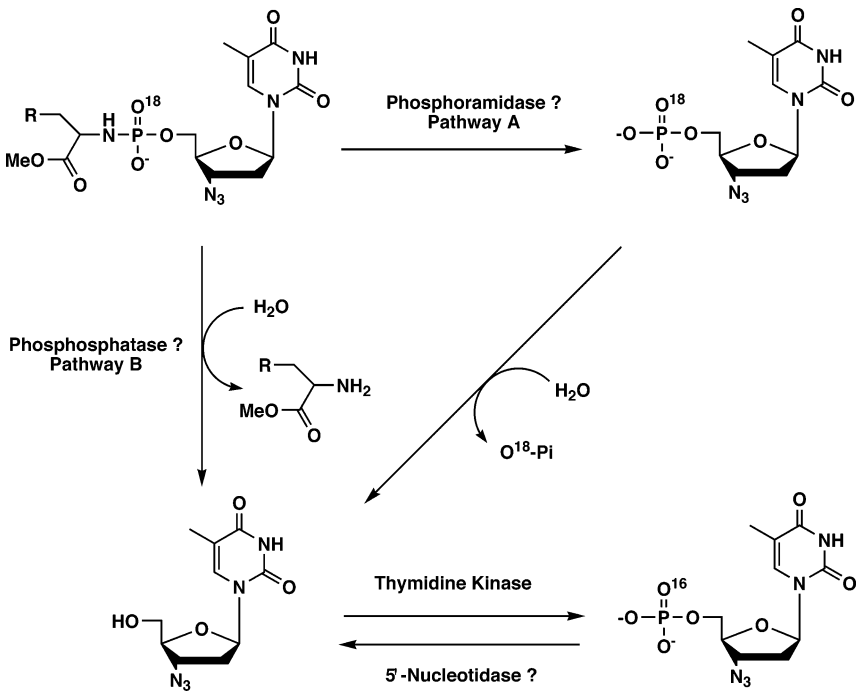

Figure 1. Proposed intracellular decomposition pathways of AZT amino acid phosphoramidate.

decreased activity of the prerequisite first phosphorylating enzyme.

In principle, the problem of inefficient cellular nucleoside phosphorylation could be overcome by the use of nucleoside monophosphates (NMPs). Unfortunately, NMPs are not metabolically stable *in vivo*, and they are incapable of crossing cellular membranes since they carry a charge of −2 at physiological pH. To address this challenge, several clever prodrug or "pronucleotide" approaches have been devised for the intracellular delivery of NMPs.[7,8]

Nucleoside amino acid phosphoramidate monoesters have shown promise as a potential pronucleotide strategy.[8] In particular, we have demonstrated that 3′-azido-3′-deoxythymidine (AZT) amino acid phosphoramidates are potent, nontoxic antiviral, and/or anticancer agents.[9−13] AZT phosphoramidates are readily taken up by lymphocytic and breast cancer tumor tissue and converted to the corresponding AZT monophosphate (AZT-MP).[13] Cell extract studies have provided evidence of a bioactivation mechanism that relies on enzyme-catalyzed P−N bond hydrolysis (Figure 1, pathway A).[12,14−16] Nevertheless, the intracellular conversion of AZT phosphoramidates to AZT-MP could proceed by P−O bond cleavage followed by AZT rephosphorylation (Figure 1, pathway B). Subsequent phosphorylation of AZT-

(2) Antonelli, G.; Turriziani, O.; Verri, A.; Narciso, P.; Ferri, F.; D'Offizi, G.; Dianzini, F. Long-term exposure to zidovudine affects in vitro and in vivo the efficiency of thymidine kinase. *AIDS Res. Hum. Retroviruses* **1996**, *12*, 223−228.
(3) Hoever, G.; Groeschel, B.; Chandra, P.; Doerr, H. W.; Cinatl, J. The mechanism of 3′-azido-2′,3′-dideoxythymidine resistance to human lymphoid cells. *Int. J. Mol. Med.* **2003**, *11*, 743−747.
(4) Magnani, M.; Gazzanelli, G.; Brandi, G.; Casabianca, A.; Fraternale, A.; Chiarantini, L.; Rossi, L. 2′,3′-Dideoxycytidine-induced drug resistance in human cells. *Life Sci.* **1995**, *57*, 881−887.
(5) Darby, G.; Field, H. J. Altered substrate specificity of herpes simplex virus thymidine dinase confers acyclovir resistance. *Nature* **1981**, *289*, 81−83.
(6) Suzutani, T.; Shioka, K.; De Clercq, E.; Ishibashi, K.; Kaneko, H.; Kira, T.; Hashimoto, K.; Ogasawara, M.; Ohtani, K.; Wakamiya, N.; Saijo, M. Differential mutation patterns in thymidine kinase and DNA polymerase genes of herpes simplex virus type 1 clones passaged in the presence of acyclovir or penciclovir. *Antimicrob. Agents Chemother.* **2003**, *47*, 1707−1713.
(7) Meier, C. Pronucleotides: recent advances in the design of efficient tools for the delivery of biologically active nucleoside monophosphates. *Synth. Lett.* **1998**, 233−242.
(8) Wagner, C. R.; Iyer, V. V.; McIntee, E. J. Pronucleotides: Toward the in vivo delivery of antiviral and anticancer nucleotides. *Med. Res. Rev.* **2000**, *20*, 417−451.
(9) Abraham, T. W.; Wagner, C. R. A phosphoramidate-based synthesis of phosphoramidate amino acid diesters of antiviral nucleosides. *Nucleosides Nucleotides Nucleic Acids* **1994**, *13*, 1891−1903.
(10) Wagner, C. R.; Chang, S.-l.; Griesgraber, G. W.; Song, H.; McIntee, E. J.; et al. Antiviral nucleoside drug delivery via amino acid phosphoramidates. *Nucleosides Nucleotides Nucleic Acids* **1999**, *18*, 913−919.
(11) McIntee, E. J.; Remmel, R. P.; Schinazi, R. F.; Abraham, T. W.; Wagner, C. R. Probing the mechanism of action and decomposition of amino acid phosphomonoester amidates of antiviral nucleoside prodrugs. *J. Med. Chem.* **1997**, *40*, 3323−3331.
(12) Chang, S.-l.; Griesgraber, G. W.; Southern, P. J.; Wagner, C. R. Amino acid phosphoramidate monoesters of 3′-azido-3′-deoxythymidine: Relationship between antiviral potency and intracellular metabolism. *J. Med. Chem.* **2001**, *44*, 223−231.
(13) Iyer, V. V.; Griesgraber, G. W.; Radmer, M. R.; McIntee, E. J.; Wagner, C. R. Synthesis, in Vitro anti-breast cancer activity, and intracellular decomposition of amino acid methyl ester and alkyl amide phosphoramidate monoesters of 3′-azido-3′-deoxythymidine (AZT). *J. Med. Chem.* **2000**, *43*, 2266−2274.

MP from either pathway will lead to the formation of AZT-DP and AZT-TP.

To distinguish between these two mechanistic possibilities, the biological activity (i.e., antiviral or anticancer potency) of a pronucleotide is typically determined with a kinase deficient cell line. For example, phosphoramidate diesters of 2′,3′-didehydrothymidine (D4T) have been shown to be more effective inhibitors than D4T of the replication of HIV by lymphocytic cells deficient in thymidine kinase (TK−) activity.[17] These results were found to be consistent with the increased amount, relative to D4T, of intracellular D4T-MP observed for TK− cells treated with the prodrug.[18,19] While the use of a biological end point in combination with kinase deficient cells has been informative, pronucleotide efficacy cannot be determined for normal tissues or cells in which kinase deficient cell lines are not available. Additional genetic changes can also accompany the development of kinase deficient cell lines, resulting in differential expression of organic anion exporters and nucleotidases capable of depleting cells of nucleoside monophosphates.[21,22] Since AZT phosphoramidates have been shown to be substrates for a putative phosphoramidase and AZT-MP is poorly converted to AZT-DP and AZT-TP, we chose to investigate the potential utility of monitoring the intracellular fate of an ^{18}O-labeled phosphoramidate pronucleotide by LC−ESI$^-$-MS/MS.

Materials and Methods

AZT was kindly donated by Toronto Research Chemicals Inc. (North York, ON). Trimethyl phosphate (TMP), ethylenediaminetetraacetic acid (EDTA, free acid), and 4-morpholineethanesulfonic acid monohydrate (MES) were purchased from Fisher. Sodium 2,2-dimethyl-2-silapentane-5-sulfonate (DSS) was purchased from Cambridge Isotope Laboratory Inc. AZT-MP was synthesized according to the published procedure.[22,23] 4-(2-Hydroxyethyl)-1-piperazineethanesulfonic acid (HEPES), *N*,*N*-dimethylhexylamine (DMHA), and formic acid were purchased from Sigma-Aldrich. RPMI-1640, fetal bovine serum (FBS), and trypan blue stain (0.4%) in saline (0.85%) were purchased from Gibco (Grand Island, NY). Sterile stock solutions of penicillin G, streptomycin, human interleukin-2, and phytohemagglutinin have been prepared with sterilizing filters. Solvents used for LC analyses are HPLC gradient-grade. All the solutions for instrumental analyses were filtered through a 0.22 μm membrane filter, and degassed prior to being loaded on the column.

Synthesis and Characterization of [^{18}O]2. The preparation of ^{18}O-incorporated triethylammonium 3′-azido-3′-deoxythymidine 5′-phosphite (AZT H-phosphonate) was carried out as follows. To a solution of diphenyl phosphite (400 μL, 1.7 mmol) in 3 mL of pyridine under argon was added dropwise a solution of AZT (910 mg, 3.4 mmol) in 5 mL of pyridine for 40 min. After the mixture had been stirred for 2 h at room temperature, triethylamine (550 μL) and $H_2{}^{18}O$ (550 μL, 95% ^{18}O-enriched) were added. After additional stirring overnight, the mixture was submitted to the reduced pressure to be concentrated. The residue above was dissolved in H_2O and extracted with CH_2Cl_2 (three times). The aqueous fraction was concentrated, and the residue was submitted to flash chromatography (5/2/0.25 $CHCl_3$/MeOH/H_2O mixture with 1% NH_4OH) to give a purified AZT H-phosphonate (650 mg, 88% yield, 80% incorporation of ^{18}O into the P═O bond).

The synthesis of [^{18}O]**2** was carried out as follows. To a solution of ^{18}O-incorporated triethylammonium 3′-azido-3′-deoxythymidine 5′-phosphite (300 mg, 0.7 mmol) in 14 mL of dry pyridine was added TMSCl (350 μL, 2.7 mmol) under argon. After 5 min, a solution of I_2 (300 mg, 1.2 mmol) was added dropwise, and the addition of the solution was stopped when the disappearance of I_2 was complete. After 5 min, triethylamine (1 mL) followed by L-tryptophan methyl ester

(14) Abraham, T. W.; Kalman, T. I.; McIntee, E. J.; Wagner, C. R. Synthesis and biological activity of aromatic amino acid phosphoramidates of 5-fluoro-2′-deoxyuridine and 1-β-arabinofuranosylcytosine: evidence of phosphoramidase activity. *J. Med. Chem.* **1996**, *39*, 4569−4575.

(15) Wagner, C. R.; McIntee, E. J.; Schinazi, R. F.; Abraham, T. W. Aromatic amino acid phosphoramidate di- and triesters of 3′-azido-3′-deoxythymidine (AZT) are non-toxic inhibitors of HIV-1 replication. *Bioorg. Med. Chem. Lett.* **1995**, *5*, 1819−1824.

(16) Abraham, T. W.; McIntee, E. J.; Iyer, V. V.; Schinazi, R. F.; Wagner, C. R. Synthesis, biological activity and decomposition studies of amino acid phosphomonoester amidates of acyclovir. *Nucleosides Nucleotides Nucleic Acids* **1997**, *16*, 2079−2092.

(17) McGuigan, C.; Cahard, D.; Sheeka, H. M.; De Clercq, E.; Balzarini, J. Aryl phosphoramidate derivatives of d4T have improved anti-HIV efficacy in tissue culture and may act by the generation of a novel intracellular metabolite. *J. Med. Chem.* **1996**, *39*, 1748−1753.

(18) Balzarini, J.; Karlsson, A.; Aquaro, S.; Perno, C.-F.; Cahard, D.; Naesens, L.; De Clercq, E.; McGuigan, C. Mechanism of anti-HIV action of masked alaninyl d4T-MP derivatives. *Proc. Natl. Acad. Sci. U.S.A.* **1996**, *93*, 7295−7299.

(19) Balzarini, J.; Egberink, H.; Hartmann, K.; Cahard, D.; Vahlenkamp, T.; Thormar, H.; De Clercq, E.; McGuigan, C. Antiretrovirus specificity and intracellular metabolism of 2′,3′-didehydro-2′,3′-dideoxythymidine (stavudine) and its 5′-monophosphate triester prodrug So324. *Mol. Pharmacol.* **1996**, *50*, 1207−1213.

(20) Balzarini, J.; Naesens, L.; Aquaro, S.; Knispel, T.; Perno, C. F.; De Clercq, E.; Meier, C. Intracellular metabolism of CycloSaligenyl 3′-azido-2′,3′-dideoxythymidine monophosphate, a prodrug of 3′-azido-2′,3′-dideoxythymidine (zidovudine). *Mol. Pharmacol.* **1999**, *56*, 1354−1361.

(21) Schuetz, J. D.; Connelly, M. C.; Sun, D. X.; Paibir, S. G.; Flynn, P. M.; Srinivas, R. V.; Kumar, A.; Fridland, A. MRP4: A previously unidentified factor in resistance to nucleoside-based antiviral drugs. *Nat. Med.* **1999**, *5*, 1048−1051.

(22) Schott, H.; Ludwig, P. S.; Immelmann, A.; Schwendener, R. A. Synthesis and in vitro anti-HIV activities of amphiphilic heterodinucleoside phosphate derivatives containing the 2′,3′-dideoxynucleosides ddC, AZT and ddI. *Eur. J. Med. Chem.* **1999**, *34*, 343−352.

(23) Glinski, R. P.; Khan, M. S.; Kalamas, R. L.; Sporn, M. B. Nucleotide synthesis. IV. Phosphorylated 3′-amino-3′-deoxythymidine and 5′-amino-5′-deoxythymidine and derivatives. *J. Org. Chem.* **1973**, *38*, 4299−4305.

hydrochloride (400 mg, 1.6 mmol) was added to the reaction mixture. After being stirred for an additional 15 min, the reaction mixture was concentrated under reduced pressure. The residue was partitioned between H_2O and CH_2Cl_2. The aqueous fraction was concentrated, and the residue was applied to an Amberlite (IRP-64) ion exchange column. The pooled fraction above was concentrated, and the residue was submitted to flash chromatography (5/2/0.25 $CHCl_3$/MeOH/H_2O mixture with 1% NH_4OH) to give purified [^{18}O]**2** (280 mg, 71% yield, 55% incorporation of ^{18}O into the P═O bond).

The characterization of ^{18}O incorporation was carried out with ^{31}P NMR by employing the deconvolution analysis. The ^{31}P NMR data were collected at 25 °C on a Varian Inova 600 MHz spectrometer at a frequency of 243 MHz in the gated proton decoupling mode. The Varian NMR software allowed the deconvolution of observed spectra into individual Gaussian lines for the integration of multiply overlapped peaks: ^{1}H NMR (D_2O, 300 MHz) δ 7.22 (d, J = 8.0 Hz, 1H), 7.10 (d, J = 8.0 Hz, 1H), 7.06 (s, 1H), 6.91 (s, 1H), 6.86 (t, J = 7.8 Hz, 1H), 6.73 (t, J = 7.7 Hz, 1H), 5.69 (t, J = 6.5 Hz, 1H), 3.89 (m, 1H), 3.77 (m, 1H), 3.64 (m, 1H), 3.53 (2H), 3.45 (s, 3H), 2.89 (m, 1H), 2.77 (m, 1H), 1.86 (m, 1H), 1.63 (m, 1H), 1.50 (s, 3H); ^{31}P NMR (D_2O, MES buffer at pH 6.65, 243 MHz) δ 7.23 ([^{18}O]ATO), 7.26 ([^{16}O]ATO); ^{13}C NMR (CD_3OD) δ 11.7, 30.7, 30.8, 36.9, 51.3, 56.0, 61.6, 64.2, 83.6, 84.6, 109.8, 110.9, 111.9, 118.2, 118.4, 121.2, 123.3, 127.7, 136.7, 151.1, 165.1, 175.5.

Culture of Cells. CCRF-CEM cells [human T-lymphoblastoid leukemia cell lines that were purchased from American Type Culture Collection (Manassas, VA)] were cultured in RPMI 1640 medium supplemented with 20% heat-inactivated fetal bovine serum, penicillin G (Fisher) (100 units/mL), streptomycin (Sigma) (10 μg/mL), and human interleukin-2 (IL-2) (Boehringer Mannheim) (10 units/mL).

PBMC cells were kindly donated by Dr. Balfour's group in AIDS Clinical Trials Unit (ACTU) in the Department of Laboratory Medicine and Pathology at the University of Minnesota and cultured in RPMI 1640 medium supplemented with 10% heat-inactivated fetal bovine serum, penicillin G (100 units/mL), and streptomycin (100 μg/mL). Cultures were supplemented with phytohemagglutinin (PHA, Sigma) (10 μg/mL) and IL-2 (10 units/mL).

Incubation of Cells with [^{18}O]2. Cells were suspended in a tissue culture flask at a density of 10^6 cells/mL in fresh growth medium. For each experiment, 5 million cells were incubated with a known concentration of [^{18}O]**2** in a 10% CO_2/90% air atmosphere at 37 °C. At various time intervals, cells were counted using the trypan blue dye exclusion method and were centrifuged to form a cell pellet (1500 rpm for 10 min at 20 °C). The supernatant was removed, and the cell pellet was treated with an ice-cold 60% methanol/40% 15 mM ammonium acetate buffer (pH 6.65). The residue above was set at −20 °C overnight and then lyophilized. To the dried cell extract above, was added 100 μL of 20 mM HEPES (pH 7.2). This sample was then diluted 250−1000 times for AZT-MP analyses and 250−4000-fold for prodrug analyses. The intracellular concentrations of AZT-MP and **2** reported in this paper represent the value per 1 million cells, which were the converted values using the appropriate dilution factors. To the sample above were added internal standards (D4T and L-DPO) before submission to the LC−MS instrument. To prevent the contamination of the LC column and MS detector by salts and most cellular residues, an online switching method was employed.

HPLC Method. Chromatographic separation was achieved using a capillary Zorbax XDB-C18 column (150 mm × 0.5 mm, 5 μm, Agilent Technologies) eluted at a flow rate of 12 μL/min. An injection volume of 5 μL was used for standard samples as well as cell extract samples. The mobile phase was composed of solvents A and B. Solvent A was 15 mM ammonium acetate (pH 6.65), and solvent B was methanol. Two different gradient systems were used: one for analyzing metabolites and the other for analyzing [^{18}O/^{16}O]**2**. The gradient condition for metabolites was as follows: 0 to 15% MeOH from 0 to 5 min, 15 to 50% MeOH from 5 to 25 min, and 50 to 85% MeOH from 25 to 30 min. Column washing with 100% A was performed over the course of 5 min, and the equilibration time before the next analysis was set at 12 min. The gradient condition for [^{18}O/^{16}O]**2** was as follows: 60 to 70% MeOH from 0 to 6 min, 70 to 75% MeOH from 6 to 9 min, and 75 to 82% MeOH from 9 to 10 min. The column temperature was maintained at 24 °C using a thermostated column compartment. To minimize salt contamination, HPLC effluent from the first 3−7 min of each run was diverted to waste utilizing an online column switching mode.

Capillary HPLC−ESI$^-$-MS/MS Analysis. An Agilent (Wilmington, DE) 1100 capillary LC−ion trap MS system was used for the analyses. The details of chromatographic separation were discussed above. The mass spectrometer was operated in the negative ion mode with nitrogen as a nebulizing and drying gas (15 psi, 5 L/min). The total eluent flow of 12 μL/min was directed to the ESI source. The HV capillary voltage was set to 3100−4311 V. The drying gas temperature was set to 200 °C. The capillary exit voltage was −131 V. ESI source parameters and MS/MS parameters were optimized for maximum sensitivity during direct infusion of authentic standards. Quantitation and identification of prodrugs and metabolites by HPLC−ESI$^-$-MS/MS were carried out with the Chemstation software (Agilent).

Measurement of the Intracellular Concentration of [^{18}O/^{16}O]AZT-MP. The negative ion ESI and selective multiple-reaction monitoring (MRM) mode was used for analyses of metabolites of [^{18}O/^{16}O]**2** in the sample. The MS experiment was divided into three segments to detect each analyte at a different retention time: 0−12 min for [^{18}O/^{16}O]AZT-MP, 12−17 min for D4T, and 17−25 min for AZT. The HV capillary voltage was set to 4311 V. The parent ion of each analyte (m/z 346.5 for [^{16}O]AZT-MP, m/z 348.5 for [^{18}O]AZT-MP, and m/z 265.0 for AZT) was trapped and fragmented simultaneously by using an isolation width of 1 mass unit (mu).

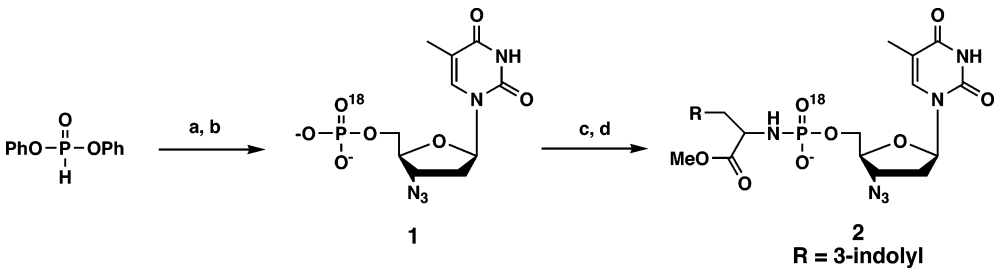

Figure 2. Synthesis of [^{18}O]**2**: (a) AZT (2 equiv), pyridine; (b) triethylamine, $H_2{}^{18}O$; (c) TMSCl (3 equiv), pyridine, I_2; ^{d}L-tryptophan methyl ester, triethylamine (2 equiv).

The procedure for quantitation of [^{18}O/^{16}O]AZT-MP was carried out as follows. The [M − H]$^-$ ions of [^{16}O]AZT-MP (*m*/*z* 346.0), [^{18}O]AZT-MP (*m*/*z* 348.0), and the internal standard, D4T (*m*/*z* 223.0), were isolated and subjected to collision-induced dissociation (CID, fragmentation amplitude = 1.0). The product ions were detected within the scan range of *m*/*z* 100−400. The target ion abundance value was 30 000, and the maximum accumulation time was 300 ms. The instrument was tuned to maximize sensitivity during the infusion of a standard solution of authentic AZT-MP. [^{16}O]AZT-MP was quantitated from fragment ions at *m*/*z* 125, 177, 303, and 346. [^{18}O]AZT-MP was quantitated from fragment ions at *m*/*z* 125, 179, 305, and 348. The D4T internal standard was analyzed analogously based on fragment ions at *m*/*z* 125, 150, 193, and 223. Calibration curves were constructed by injecting standard solutions containing known amounts of AZT-MP and D4T, followed by analysis of the HPLC−ESI$^-$-MS/MS peak area ratios. Then quantitative analyses were carried out on the basis of the ratio of the peak area in the selected ion chromatogram corresponding to AZT-MP to the peak area of D4T (relative response factors). The linearity was checked using calibration graphs for AZT-MP using six standard solution samples.[24−26]

The procedure for quantitation of AZT was carried out as follows. The [M − H]$^-$ ions of AZT (*m*/*z* 265) and the D4T internal standard (*m*/*z* 223) were isolated and subjected to collision-induced dissociation (CID, fragmentation amplitude = 1). The product ions were detected within the scan range of *m*/*z* 100−300. The target ion abundance value was 30 000, and the maximum accumulation time was 300 ms. AZT was quantitated from the fragment ion at *m*/*z* 223. The D4T internal standard was analyzed analogously based on fragment ions at *m*/*z* 125, 150, 193, and 223. Calibration curves were constructed by injecting standard solutions containing known amounts of AZT (2, 5, 10, and 20 pmol) and D4T (10 pmol), followed by analysis of the HPLC−ESI$^-$-MS/MS peak area ratios. Then quantitative analyses were carried out on the basis of the ratio of the peak area in the selected ion chromatogram corresponding to AZT to the peak area of D4T (relative response factors). The linearity of the relative response was checked using calibration graphs and four standard solution samples of AZT.

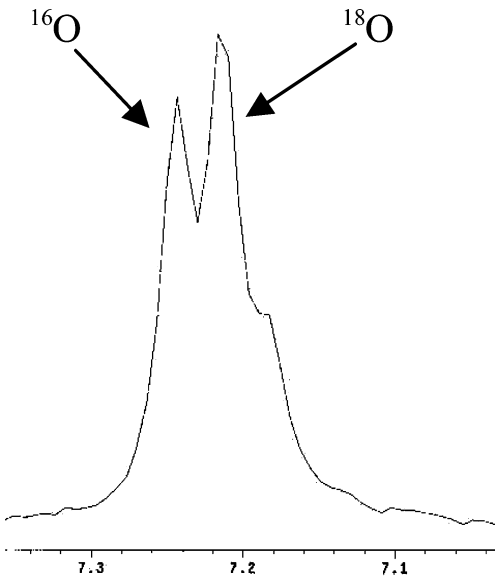

Figure 3. ^{31}P NMR spectrum of [^{18}O]**2**.

Measurement of the Intracellular Concentration of [^{18}O/^{16}O]2. The negative ion ESI and selective multiple-reaction monitoring (MRM) mode was used for analyses of [^{18}O/^{16}O]**2** in the sample. The MS experiment was divided into two segments to detect each analyte at a different retention time: 0−6 min for L-DPO and 6−9 min for [^{18}O/^{16}O]-**2**. The HV capillary voltage was set to 3500 V for the first segment and 3100 V for the second segment. The parent ion of each analyte (*m*/*z* 546.5 for [^{16}O]**2** and *m*/*z* 548.5 for [^{18}O]**2**) was trapped and fragmented simultaneously by using an isolation width of 1 mass unit (mu). Parent prodrugs [^{16}O]**2** (*m*/*z* 546.5) and [^{18}O]**2** (*m*/*z* 548.5) were quantitated in a manner similar to that of [^{18}O/^{16}O]AZT-MP. The [M − H]$^-$ ions of [^{16}O]**2** (*m*/*z* 546.5), [^{18}O]**2** (*m*/*z* 548.5), and the L-DPO internal standard (*m*/*z* 464.5) were isolated in the two different sections and subjected to collision-induced dissociation (CID, fragmentation amplitude = 0.85). The product ions were detected within the scan range of *m*/*z* 100−700. The target ion abundance value was 1000 for [^{18}O/^{16}O]**2** and 30 000 for L-DPO, and the maximum accumulation time was 300 ms. [^{18}O]**2** was quantitated from

(24) Dass, C. *Principles and practice of biological mass spectrometry*; John Wiley & Sons: New York, 2001.
(25) Roboz, J. *Mass spectrometry in cancer reserach*; CRC Press: Boca Raton, FL, 2002.
(26) Siuzdak, G. *Mass spetrometry for biotechnology*; Academic Press: San Diego, 1996.

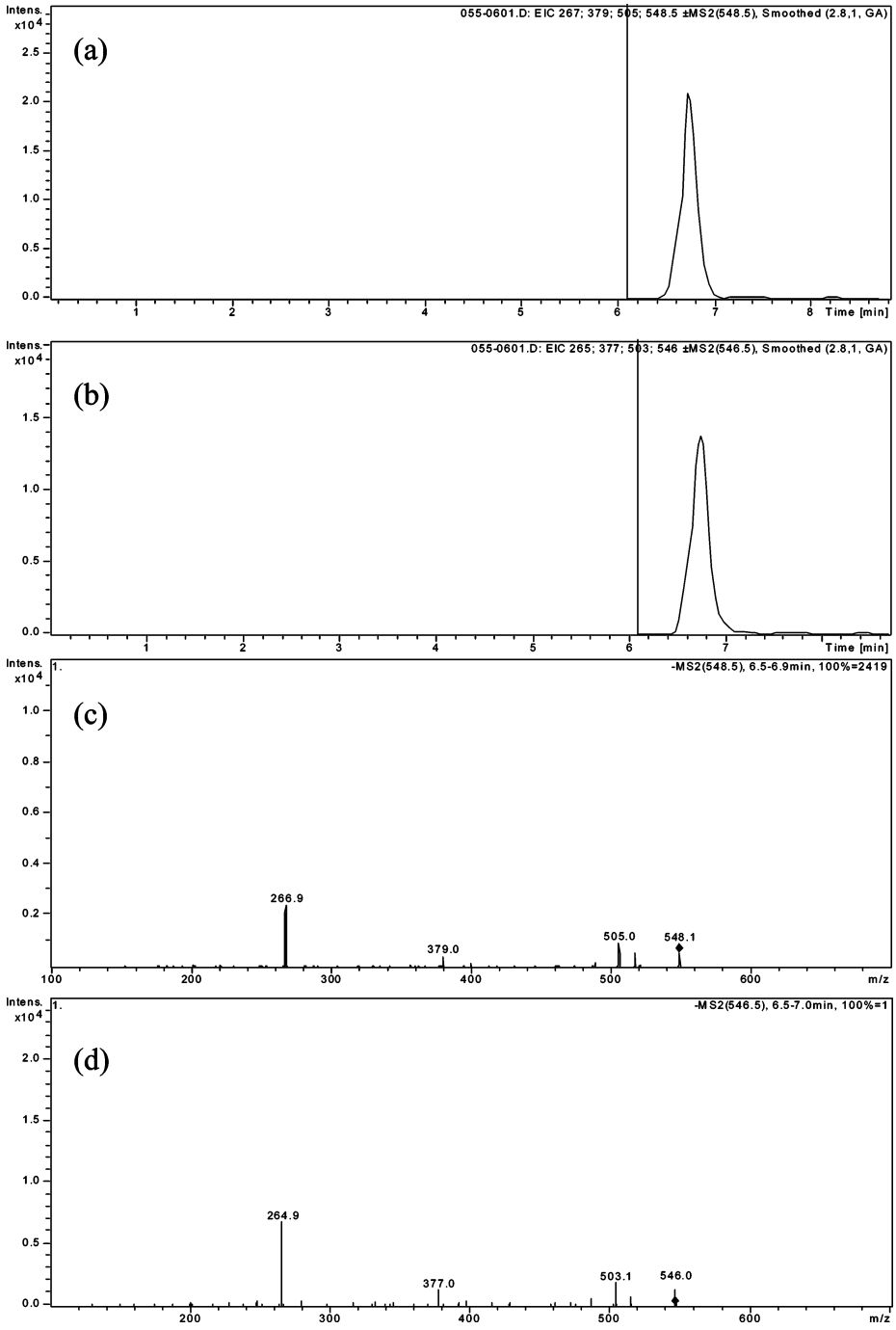

Figure 4. Representative extracted ion chromatogram of (a) [^{18}O]**2** in a standard sample and (b) [^{16}O]**2**. ESI$^-$-MS/MS spectrum of (c) [^{18}O]**2** in a standard sample and (d) [^{16}O]**2**.

fragment ions at *m*/*z* 267, 379, 505, and 548. [^{16}O]**2** was quantitated from fragment ions at *m*/*z* 265, 377, 503, and 546. The L-DPO internal standard was analyzed analogously on the basis of fragment ions at *m*/*z* 279, 338, and 464. Calibration curves were constructed by injecting standard solutions containing known amounts of total **2** ([^{18}O]- and [^{16}O]**2**) and L-DPO, followed by analysis of the HPLC−ESI$^-$-MS/MS peak area ratios. Then, quantitative analyses were carried out on the basis of the ratio of the area of the peak in the selected ion chromatogram corresponding to the prodrug to the peak area of L-DPO (relative response factors). The linearity was checked using calibration graphs for prodrugs using seven standard solution samples.

Stability Test of [^{16}O]2. [^{16}O]**2** (2.5 μmol) was dissolved in 500 μL of buffer [0.5 mM $MgCl_2$ and 20 mM HEPES (pH 7.2)] and the solution was kept at 22 °C for 4 or 20 h. At each time point, the sample above was diluted and the diluted fraction was submitted to the LC−MS instrument. The LC−MS/MS analysis was carried out as described above.

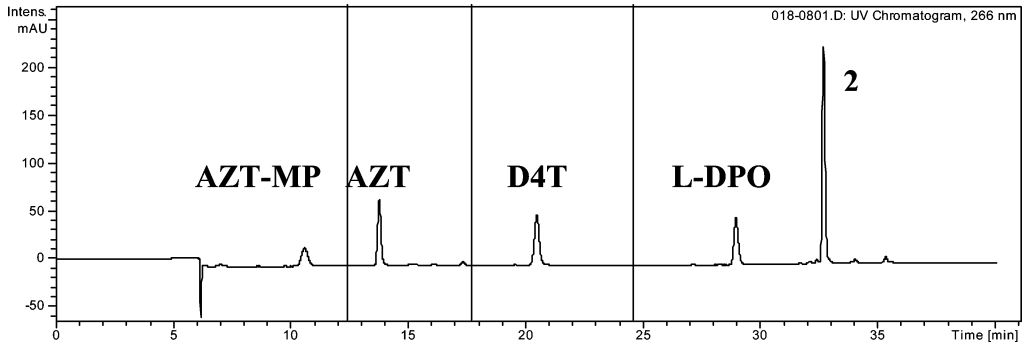

Figure 5. Representative capillary RP-HPLC chromatogram of a standard sample containing authentic AZT-MP, D4T, AZT, L-DPO, **2**, AMP, ADP, and ATP (adenosine phosphates were eluted with solvent front). Solvent A was 15 mM ammonium acetate (pH 6.65), and solvent B was methanol. Gradient: 0 to 15% MeOH from 0 to 5 min, 15 to 50% MeOH from 5 to 25 min, 50 to 85% MeOH from 25 to 30 min, and 85 to 87% MeOH from 30 to 40 min at a flow rate of 12 μL/min.

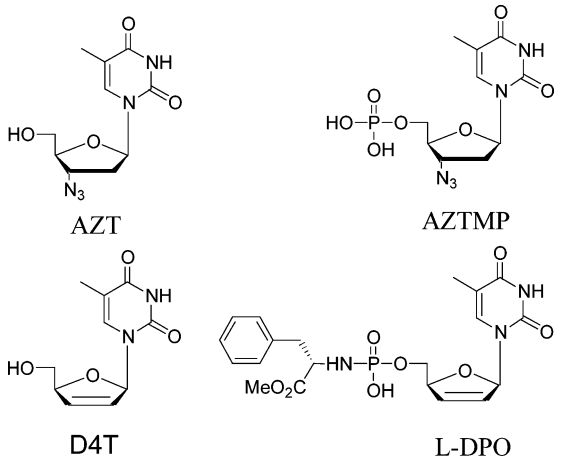

Figure 6. Structures of AZT, AZT-MP, D4T, and L-DPO.

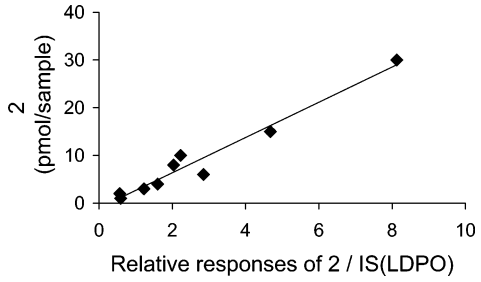

Figure 7. Representative standard curve for [^{18}O]**2** and internal standard IS (L-DPO).

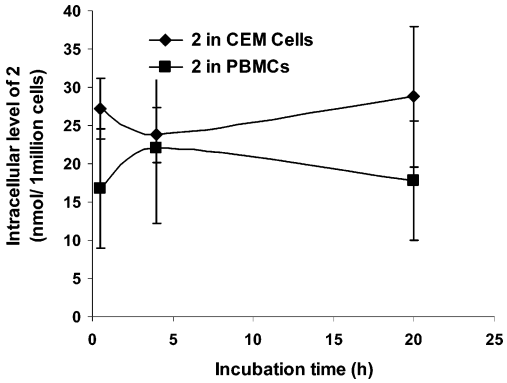

Figure 8. Intracellular amounts of [^{18}O]- and [^{16}O]**2** in CEM cells (◆) and PBMCs (■). Cells were incubated for various amounts of time at 37 °C with an [^{18}O]**2** concentration of 2.5 mM.

Results and Discussion

Chemistry. To synthesize ^{18}O-incorporated AZT L-tryptophan methyl ester phosphoramidate, a strategy utilizing H-phosphonate chemistry was employed (Figure 2).[12,13] In the first step, the addition of AZT to diphenyl phosphite followed by the addition of triethylamine·$H_2{}^{18}O$ yielded AZT H-phosphonate, **1**, in 88% with 80% incorporation of ^{18}O, as determined by deconvolution of the ^{31}P NMR spectra (data not shown). The synthesis of [^{18}O]AZT L-tryptophan methyl ester phosphoramidate, **2**, was completed by treatment of the H-phosphonate, **1**, with trimethylsilyl chloride (TMSCl) and iodine (I_2) followed by addition of L-tryptophan methyl ester.[12,13] The final product **2** was isolated with a yield of 71% and found by ^{31}P NMR spectra analysis and LC−MS to be 55% enriched with ^{18}O (Figure 3). The loss of label probably resulted from the highly hygroscopic nature of **1**.

Analysis of **2** by LC−ESI$^-$-MS/MS revealed a single peak at the extracted ion chromatography (EIC) (Figure 4a,b), in which both [^{18}O]**2** and [^{16}O]**2** products could be easily resolved by MS/MS (Figure 4c,d). The [M − H]$^-$ ion (*m*/*z* 548) for [^{18}O]**2** was shown to be exactly 2 mu greater than that for [^{16}O]**2** (*m*/*z* 546). In addition, the extracted fragment ions for *m*/*z* 505 (−N_3 − H), *m*/*z* 379 (−thymine − N_3 − H), and *m*/*z* 267 (−OMe − $C_{10}H_{11}N_5O_3$) are consistent with the corresponding fragments from [^{16}O]**2** (*m*/*z* 503, 377, and 265). Fragmentation of the phosphoramidate C−O bond is apparently preferred to fragmentation of the P−N bond. Whether this is due to unique fragmentation properties of AZT-based phosphoramidates or is a general property of nucleoside phosphoramidates remains to be determined.

Assay Development. With the labeled phosphoramidate, [^{18}O]**2**, in hand, assay validation studies were conducted. The HPLC conditions that were used were able to fully resolve AZT, AZT-MP, **2**, and the internal standards with little or no contamination by AMP, ADP, and ATP which are abundant in cells (Figure 5). For the detection of intracellular

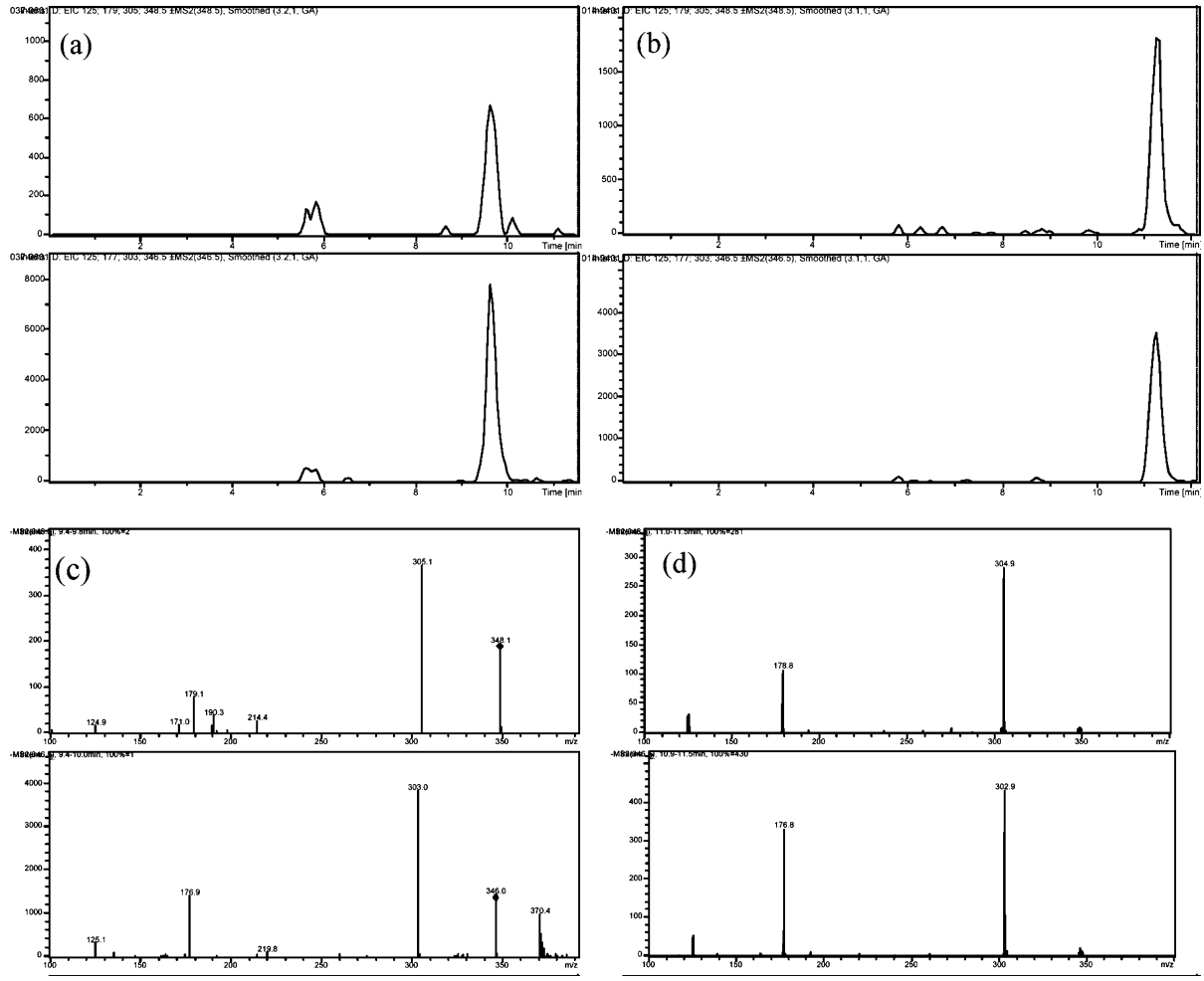

Figure 9. Extracted ion chromatogram of [^{18}O]AZT-MP and [^{16}O]AZT-MP in (a) CEM cells incubated with 2.5 mM [^{18}O]**2** for 20 h and (b) PBMCs under the same condition. (c) ESI$^-$-MS/MS spectrum of [^{18}O]AZT-MP and [^{16}O]AZT-MP in (c) CEM cells incubated with 2.5 mM [^{18}O]**2** for 20 h and (d) PBMCs under the same condition.

phosphoramidates ([^{18}O]**2** and [^{16}O]**2**) and the metabolites ([^{18}O]AZT-MP and [^{16}O]AZT-MP), full scan MS/MS in the negative ion electrospray ionization mode (ESI$^-$-MS/MS) was employed to generate fragment ions necessary for the identification of the analytes, [^{18}O]**2** and [^{16}O]**2**, [^{18}O]AZT-MP and [^{16}O]AZT-MP, and AZT, as well as the internal standards, D4T and L-DPO (Figure 6). Figure 7 is a representative standard curve for [^{18}O]**2** and [^{16}O]**2** and the L-DPO internal standard in HEPES buffer (pH 7.2). Linearity was observed over a range of 1−30 pmol of the phosphoramidate. By extraction of ions in the multiple-reaction monitoring mode, 55 ± 4% (n = 9) of **2** was found to be labeled with ^{18}O. This percentage is consistent with the value found previously by ^{31}P NMR analysis. Both the EIC chromatographic behavior and ESI$^-$-MS/MS spectra for [^{18}O]**2** and [^{16}O]**2** incubated with cell extract samples were found to be identical to those observed for standard samples dissolved in HEPES buffer (pH 7.2) (data not shown).

Cell Culture Studies. Before cellular incubation experiments were conducted with [^{16}O]**2**, the stability of the phosphoramidate in dilution buffer [0.5 mM $MgCl_2$ and 20 mM HEPES (pH 7.2)] was evaluated. Significant amounts of AZT or AZT-MP were not observed by LC−MS/MS when [^{16}O]**2** was incubated for either 4 or 20 h (data not shown). These results were consistent with previous stability studies conducted in buffer, plasma, and cell media.[27−29]

Both CEM cells and PBMCs were incubated with 2.5 mM [^{18}O]**2** for time intervals of 0.5, 4, and 20 h. As can be seen in Figure 8, steady-state levels of intracellular phosphoramidate were reached within the first hour. The relative ratio of intracellular [^{18}O]**2** to [^{16}O]**2** detected ranged from 1.13 ± 0.60 (0.5 h) to 1.70 ± 2.48 (20 h) for CEM cell extracts and from 1.17 ± 1.43 (0.5 h) to 1.33 ± 3.13 (20 h) for PBMC extracts (Figure 8). These values are not significantly

(27) Ballatore, C.; McGuigan, C.; De Clercq, E.; Balzarini, J. Synthesis and evaluation of novel amidate prodrugs of PMEA and PMPA. *Bioorg. Med. Chem. Lett.* **2001**, *11*, 1053−1056.

(28) Rahil, J.; Haake, P. J. Reactivity and mechanism of hydrolysis of phosphonamides. *J. Am. Chem. Soc.* **1981**, *103*, 1723−1734.

(29) Saboulard, D.; Naesens, L.; Cahard, D.; Salgado, A.; Pathirana, R.; Velazquez, S.; McGuigan, C.; DeClercq, E.; Balzarini, J. Characterization of the activation pathway of phosphoramidate triester prodrugs of stavudine and zidovudine. *Mol. Pharmacol.* **1999**, *56*, 693−704.

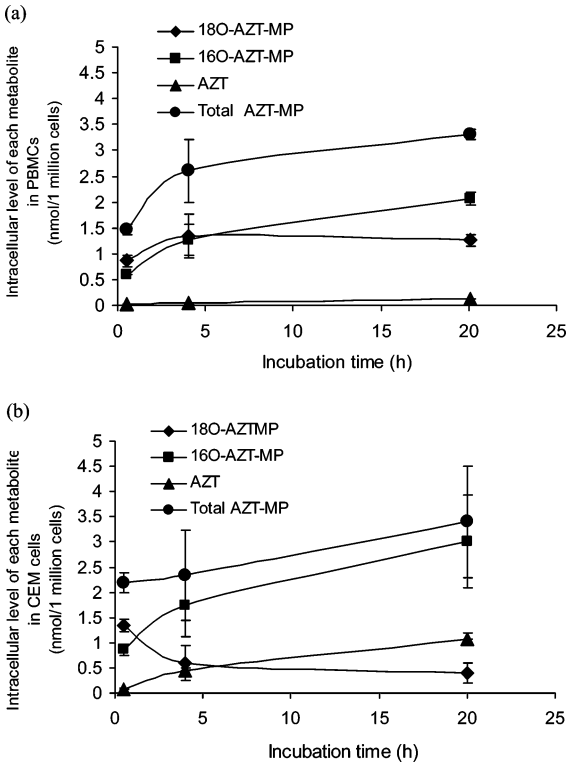

Figure 10. Intracellular amounts of total AZT-MP (●), [^{18}O]-AZT-MP (◆), [^{16}O]AZT-MP (■), and AZT (▲) in (a) PBMCs and (b) CEM cells. Cells were incubated for various amounts of time at 37 °C with an [^{18}O]**2** concentration of 2.5 mM.

different from the value of 1.22 ± 0.18 observed for standard samples, indicating little or no isotopic preference for either the cellular uptake or metabolism of [^{18}O]**2** and [^{16}O]**2**.

The EIC chromatogram (Figure 9a,b) and MS/MS spectra (Figure 9c,d) of intracellular [^{18}O]AZT-MP and [^{16}O]AZT-MP are shown after incubation with 2.5 mM [^{18}O]**2** for 20 h. As it was shown for [^{18}O]**2** and [^{16}O]**2**, the $[M - H]^-$ ion (*m*/*z* 348) for [^{18}O]AZT-MP was shown to be exactly 2 mu greater than that for [^{16}O]AZT-MP (*m*/*z* 346). In addition, the extracted fragments ions at *m*/*z* 305 ($-N_3 - H$) and *m*/*z* 179 (−thymine $- N_3 - H$) for [^{18}O]AZT-MP are consistent with the corresponding fragments at *m*/*z* 303 and 177 from [^{16}O]AZT-MP. In both cases, the nonisotopically labeled thymine fragment (*m*/*z* 125) was observed.

Examination of the conversion of [^{18}O]**2** to [^{18}O]AZT-MP and [^{16}O]AZT-MP revealed distinct similarities and differences between PBMCs and CEM cells (Figure 10a,b). For both cell types, the total amounts of intracellular AZT-MP were approximately the same, ranging from 7.5% (0.5 h) to 15% (20 h) of the intracellular phosphoramidate for PBMCs and 10% (0.5 h) to 14% (20 h) of the intracellular phosphoramidate for CEM cells. In addition, with the exception of the earliest time interval, the rate of accumulation proceeded linearly and did not reach a plateau. The discrepancy in the initial rate of phosphoramidate uptake between the two cell types is likely a reflection of cellular differences. For the initial time interval of 0.5 h, similar isotopic ratios of 1.55 ± 0.37 and 1.43 ± 0.64 were found for CEM cells and PBMCs, respectively. When compared to the ratio of 1.22 ± 0.18 for [^{18}O]**2**, phosphoramidate metabolism clearly proceeds initially by P−N and not P−O bond hydrolysis. However, for CEM cells, a rapid loss of [^{18}O]AZT-MP and an increase in the amount of AZT and [^{16}O]AZT-MP was observed (Figure 10b). From 0.5 to 4 h, the [^{18}O]AZT-MP/[^{16}O]AZT-MP ratio decreased from 1.55 ± 0.37 to 0.34 ± 0.36. In contrast, for PBMCs, the loss of [^{18}O]AZT-MP was far more gradual. For the same 0.5 and 4 h time intervals, the [^{18}O]AZT-MP/[^{16}O]AZT-MP ratio decreased only slightly from 1.43 ± 0.64 to 1.06 ± 0.64. Even at 20 h, the [^{18}O]AZT-MP/[^{16}O]AZT-MP ratio (0.61 ± 0.09) for PBMCs was approximately 2- and 5-fold greater than the values observed for CEM cells at 4 and 20 h, respectively. In addition, the rate of accumulation of AZT in CEM cells [0.124 ± 0.052 nmol (1 million cells)$^{-1}$ h^{-1}, $R^2 = 0.95$, $n = 6$] was nearly 1.4-fold greater than the rate of AZT accumulation observed for PBMCs [0.087 ± 0.0037 nmol (1 million cells)$^{-1}$ h^{-1}].

Conclusions

Taken together, the results of the cell culture studies with [^{18}O]**2** clearly revealed that direct intracellular nucleoside phosphoramidate monoester conversion to the corresponding nucleoside 5′-monophosphate can proceed via P−N bond hydrolysis (Figure 1, pathway A). However, increasing levels of intracellular AZT and the nearly complete loss of [^{18}O]-AZT-MP with time observed for incubations with CEM cells suggest that AZT-MP is particularly susceptible to dephosphorylation by one or more 5′-nucleotidases. This result is consistent with earlier studies of the metabolism of cycloSal AZT pronucleotides and therefore is probably a characteristic of the nucleoside and not the type of pronucleotide.[20] In contrast, activated PBMCs appear to express lower levels of AZT-MP 5′-nucleotidase activity, since the loss of [^{18}O]-AZT-MP and increase in the amount of AZT are considerably slower. These results are consistent with earlier decomposition studies with FuDR,[14] acyclovir,[16] FLT,[11] and AZT[12] phosphoramidates by cell extracts and offer supporting evidence for the existence of intracellular nucleoside phosphoramidases. Recently, Brenner and co-workers have demonstrated that rabbit (HINT-1) and yeast (HNT) histidine triad nucleotide binding proteins are adenosine monophosphoramidases.[30] Whether the human homologue of these enzymes or a currently unidentified phosphoramidase is responsible for AZT phosphoramidate decomposition is under investigation and will be reported in due course.

In closing, unlike existing methods that rely on kinase deficient cell lines, we have demonstrated that the use of ^{18}O labeling and LC−ESI$^-$-MS/MS can provide an effective and tissue insensitive tool for assessing the efficiency of nucleoside monophosphate delivery by a pronucleotide. The

(30) Bieganowski, P.; Garrison, P. N.; Hodawadekar, S. C.; Faye, G.; Barnes, L. D.; Brenner, C. Adenosine monophosphoramidase activity of Hint and Hnt1 supports function of Kin28, Ccl1, and Tfb3. *J. Biol. Chem.* **2002**, *277*, 10852−10860.

application of similar protocols to other types of pronucleotides should prove to be useful for the evaluation of their nucleotide delivery efficacy in a wide range of tissues.

Acknowledgment. We thank Dr. Balfour's group in ACTU in the Department of Laboratory Medicine and Pathology at the University of Minnesota for providing PBMCs. Also, we thank Dr. Natalia Y. Tretyakova at the University of Minnesota for her assistance in LC−MS. We are grateful to the Unversity of Minnesota Cancer Center for access to the capillary HPLC−ESI-MS instrument. This research is supported by NIH-NCI Grant CA 89615.

MP0340338